# Highly Emitting Neutral Dinuclear Rhenium Complexes as Phosphorescent Dopants for Electroluminescent Devices

By *Matteo Mauro, Elsa Quartapelle Procopio, Yinghui Sun, Chen-Han Chien, Daniela Donghi, Monica Panigati, Pierluigi Mercandelli,* Patrizia Mussini, Giuseppe D'Alfonso,** and *Luisa De Cola**

**A series of neutral, dinuclear, luminescent rhenium(I) complexes suitable for phosphorescent organic light emitting devices (OLEDs) is reported. These compounds, of general formula [$Re_2(\mu\text{-}Cl)_2(CO)_6(\mu\text{-}1,2\text{-diazine})$], contain diazines bearing alkyl groups in one or in both the $\beta$ positions. Their electrochemical and photophysical properties are presented, as well as a combined density functional and time-dependent density functional study of their geometry, relative stability and electronic structure. The complexes show intense green/yellow emissions in toluene solution and in the solid state and some of the complexes possess high emission quantum yields ($\phi = 0.18$–$0.22$ for the derivatives with disubstituted diazines). In butyronitrile glass, at 77 K, due to the charge transfer character of the lowest (emitting) excited state, strong blue shift of the emission is observed, accompanied by a strong increase in the lifetime values. The highest-performing emitting complex, containing cyclopentapyridazine as ligand, is tested in a polymer-based light-emitting device, with poly(9-vinylcarbazole) as matrix, as well as in a device obtained by vacuum sublimation of the complex in the 2,7-bis(diphenylphosphine oxide)-9-(9-phenylcarbazol-3-yl)-9-phenylfluorene (PCF) matrix. This represents the first example of devices obtained with a rhenium complex which can be sublimed and is solution processable. Furthermore, the emission is the bluest ever reported for electrogenerated luminescence for rhenium complexes.**

## 1. Introduction

After the seminal works of Baldo, Thompson and Forrest,[1] a large number of papers have appeared, dealing with the use of phosphorescent emitters as triplet harvesting dopants, able to increase the efficiencies of light emitting devices.[2] Iridium(III) complexes have been mainly exploited,[3] but also other transition metals have been investigated, including rhenium(I).[4,5]

The synthesis of a new family of tricarbonyl rhenium(I) complexes has recently been reported,[6] which exhibit intense photoluminescence in the range 580–620 nm, with the highest quantum yields ever reported for neutral tricarbonyl rhenium complexes (up to ca. 10%). These compounds, of general formula [$Re_2(\mu\text{-}X)_2(CO)_6(\mu\text{-diazine})$], are dinuclear and contain one bridging 1,2-diazine and two bridging ancillary ligands X (in Scheme 1 the prototypical chloro-complexes with bridging pyridazine and 4-Me-pyridazine are shown, which will be indicated here as compounds **0** and **1**). The emission arises from triplet metal-to-ligand charge-transfer

[*] Dr. P. Mercandelli
Dipartimento di Chimica Strutturale e Stereochimica Inorganica
Universitá degli Studi di Milano
Via Venezian 21, 20133 Milano (Italy)
E-mail: pierluigi.mercandelli@unimi.it
Prof. G. D'Alfonso, M. Mauro, E. Quartapelle Procopio,
Dr. D. Donghi, Dr. M. Panigati
Dipartimento di Chimica Inorganica
Universitá degli Studi di Milano
Metallorganica e Analitica "L. Malatesta"
Via Venezian 21, 20133 Milano (Italy)
E-mail: giuseppe.dalfonso@unimi.it

DOI: 10.1002/adfm.200900744

Prof. L. De Cola, Dr. Y. Sun
Westfälische Wilhelms Universität Münster
Physikalisches Institut
Mendelstrasse, 7 48149 Münster, Germany and
Center for Nanotechnology (CeNTech)
48149 Münster (Germany)
E-mail: decola@uni-muenster.de
C.-H. Chien
Department of Applied Chemistry
National Chiao Tung University
Hsinchu, 30056 (Taiwan)
Prof. P. R. Mussini
Dipartimento di Chimica Fisica ed Elettrochimica
Universitá degli Studi di Milano
Via Golgi 19, 20133 Milano (Italy)

($^3$MLCT) states. Lifetimes and emission intensities strongly vary on changing the ancillary ligands (halide[6] or hydride[7]) or the substituents on the diazines, as a result of a wide variability of the rate of non-radiative decays. Computational studies[6] indicate that the emission intensity can be correlated to an easily computable parameter, such as the instantaneous interaction energy,[8] thus showing the connection between the accessibility of radiationless relaxation pathways and the stiffness of the $Re_2$-diazine scaffold, as expected for transitions involving MLCT states. On this ground it was possible to predict that highly emitting species might be obtained on using electron rich 1,2-diazines suitably substituted in the $\beta$ positions.[9]

The present work testifies on the exactness of this prediction. In fact, we have found that the presence of alkyl substituents in both the 4 and 5 positions of the 1,2-diazines gives [$Re_2(\mu$-Cl)$_2$(CO)$_6$($\mu$-diazine)] complexes with emission quantum yields about two fold higher than their mono-substituted analogues. Furthermore, due to the good solubility and stability upon sublimation of the complexes and their reversible electrochemical behavior, we have investigated their use as component in electroluminescent devices. We report here for the first time a comparison, with the same Re(I) complex (the best emitting material) of electroluminescent devices made by sublimation and by spin coating using a polymeric matrix.

## 2. Results and discussion

### 2.1. Synthesis of Ligands and Complexes

The synthesis of the ligands involved a [4 + 2] Diels–Alder cycloaddition between 1,2,4,5-tetrazine and the proper dienofile (substituted alkyne or cyclopentene enamine, see Scheme 2).[10] The corresponding complexes [$Re_2(\mu$-Cl)$_2$(CO)$_6$($\mu$-diazine)] (**1**–**6**, Schemes 1 and 3) were obtained in good isolated yields by refluxing [ReCl(CO)$_5$] with 0.5 equiv. of the 1,2-diazine, in toluene. The complexes are stable in solution at room temperature, also in a coordinating solvent as acetonitrile, and their purity was attested by spectroscopic and elemental analysis. All the complexes display four intense bands in the $\nu$(CO) IR region, as typical of this class of compounds.[6,7] The $^1$H resonances of the ortho-hydrogens of coordinated diazines exhibit a significant downfield shift (0.3–0.6 ppm) with respect to the corresponding free diazines.[10]

### 2.2. Electrochemical Characterization

The complexes **1**–**6** were investigated by cyclic voltammetry (see Figure 1 and Table 1) and the results have confirmed the main

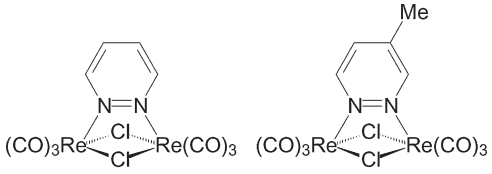


**Scheme 1.** Structures of the diazine complexes **0** and **1**.

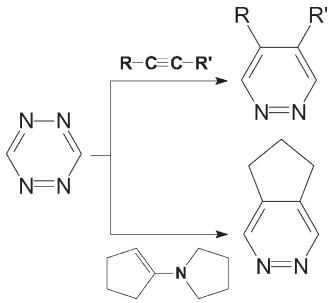


**Scheme 2.** Synthesis of the diazine ligands used in this work.

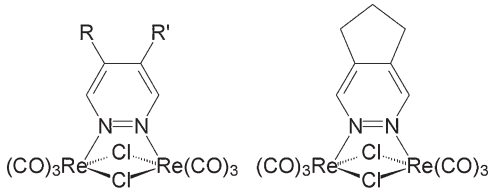


**2** R = H, R' = *n*-Hexyl
**3** R = H, R' = *t*-Bu
**4** R = Me, R' = Me
**5** R = Me, R' = *n*-Pr

**Scheme 3.** Structures of complexes **2**–**6**.

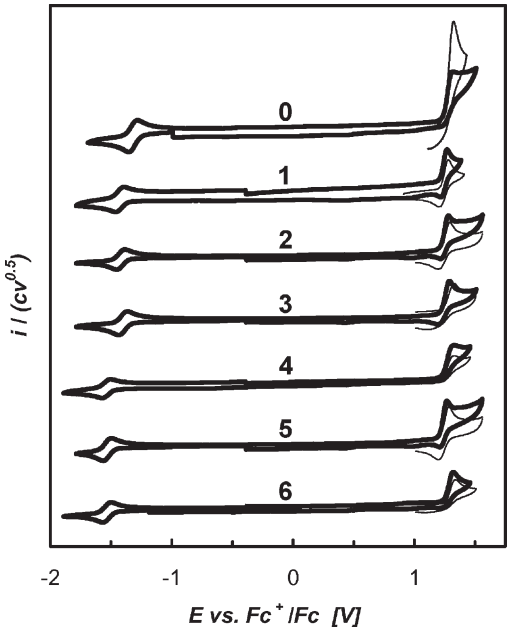


**Figure 1.** CV characteristics obtained for complexes **1**–**6** and for the analogous complex with pyridazine (compound **0**), at 0.2 V s$^{-1}$ scan rate, in MeCN, with 0.1 M $TBAPF_6$ as the supporting electrolyte, at 298 K, with ohmic drop compensation. Thick lines: CV including first oxidation and reduction peaks; thin lines: first oxidation peak at 2 V s$^{-1}$.

**Table 1.** First cathodic and anodic peak potentials ($E_{p,c}$ and $E_{p,a}$), and electrochemical ($E_g$) and UV ($E_{g,UV}$) energy gaps. Potentials are referred to the $Fc^+|Fc$ couple. The data for complexes **0** and **1** are from the previous work [6].

| Complex | $E_{p,c}$ [V] | $E_{p,al}$ [V] | $E_g$ [eV] | $E_{g,UV}$ [eV] |
|---|---|---|---|---|
| **0** | −1.345 | 1.315 | 2.66 | 3.31 |
| **1** | −1.457 | 1.271 | 2.73 | 3.41 |
| **2** | −1.460 | 1.275 | 2.74 | 3.42 |
| **3** | −1.441 | 1.290 | 2.73 | 3.42 |
| **4** | −1.583 | 1.308 | 2.89 | 3.54 |
| **5** | −1.571 | 1.267 | 2.84 | 3.50 |
| **6** | −1.571 | 1.324 | 2.90 | 3.54 |

findings of the previous study[6] on the related $[Re_2(\mu\text{-}Cl)_2(CO)_6(\mu\text{-}diazine)]$ complexes. For comparison, the data concerning the complex bearing unsubstituted pyridazine (compound **0**) are also reported in Table 1 and Figure 1. A more complete list of the electrochemical data is provided in Table S1 in the Supporting Information.

The first reduction peak, which is centered on the diazine ligand,[6] is monoelectronic and reversible, both from the chemical and the electrochemical point of view.[11] The peak potentials regularly shift in the negative direction with an increase in the number of alkyl substituents, consistently with an increasingly electron-rich aromatic site.[12]

The metal-centered oxidation corresponds to a simultaneous two-electron transfer, as in the former study,[6] according to the neatly doubled $i_L/c$ parameter with respect to the reduction peak. The process appears irreversible, both chemically and electrochemically,[13] but in the upper range of the explored scan rates return peaks emerge for some of these species (namely compounds **1**, **2**, **3**, and **5**), as shown in Figure 1. This clearly points to an (electrochemically quasi-reversible) electron transfer step and a subsequent chemical step (EC mechanism, or better $E_2C$, taking into account the bi-electronic nature of the process),[14,15] fast enough to be competitive with the reduction of the oxidation product in the backward scan. In agreement with this hypothesis, the ratio between forward and backward peak currents for complexes **1**, **2**, **3**, and **5** regularly decreases with increasing scan rate (due to the decrease of the reaction time), so that it has been possible to evaluate the pseudo-first order kinetic constants $k'_I$, that are reported in Table S1 of the Supporting Information.

Table 1 also reports the electrochemical HOMO–LUMO gaps, which regularly increase with increasing alkyl substitution, as a result of the decrease of the reduction potentials. The comparison with the spectroscopic (absorption) gaps (also reported in Table 1) is discussed in the following.

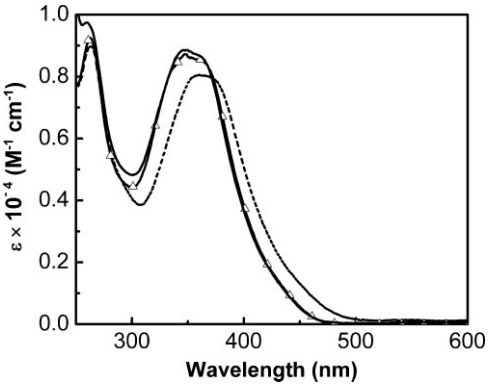


**Figure 2.** Absorption spectra of **1** (---), **4** (–△–) and **6** (—) in dichloromethane solution at room temperature.

### 2.3. Photophysical Characterization

Electronic absorption spectra for three representative complexes **1**, **4**, and **6** are depicted in Figure 2 (the others are shown in Figure S3 of the Supporting Information). Table 2 summarizes the meaningful photophysical data for all the new complexes. At room temperature, in dichloromethane solution, all the complexes show spectra dominated by two main absorption features in the UV–vis region. The intense band ($\varepsilon \approx 0.9\text{–}1.02 \times 10^4\ M^{-1}\ cm^{-1}$) at higher energy is independent of number and nature of the alkyl substituents on the pyridazine (pydz) ring and little sensitive to the solvent (Figure S4 in the Supporting Information). On the base of time-dependent density functional theory (TD DFT) computations it can be attributed to a superposition of d–d excitations from the "$t_{2g}$" set of the two Re atoms (the six HOMOs, showing a Re–Cl $\pi^*$ character[6]) to the "$e_g$" set of the two Re atoms (the LUMO + 2 to LUMO + 5 orbitals, showing in addition a large C≡O $\pi^*$ character). These transitions, being centered on the $[Re_2(\mu\text{-}Cl)_2(CO)_6]$ moiety of the complexes, do not show any significant dependence on the nature of the diazine ligand. In addition, the charge redistribution associated to these excitations does not lead to a large variation of the dipole moment of the molecule, in accord with the observed little sensitivity to the solvent of this absorption.[16]

**Table 2.** Absorption and emission spectral data of **1** – **6** at room temperature.

| | $\lambda_{abs}$ [a] [nm] ($\varepsilon 10^{-4}\ M^{-1}cm^{-1}$) | $\lambda_{em}$ [b] [nm] | $\lambda_{em}$ [c] [nm] | $\Phi$ [d] | $\tau$ [b] [μs] | $\tau$ [d] [μs] | $\tau$ [c] [μs] |
|---|---|---|---|---|---|---|---|
| **1** | 264 (0.90), 364 (0.81) | 574 | 513 | 0.08 | 0.39 | 2.0 | 34.72 |
| **2** | 263 (1.02), 363 (0.94) | 575 | 510 | 0.09 | 0.43 | 2.2 | 33.78 |
| **3** | 263 (0.92), 363 (0.87) | 573 | 505 | 0.10 | 0.43 | 2.4 | 30.90 |
| **4** | 263 (0.92), 351 (0.86) | 550 | 500 | 0.18 | 0.44 | 4.9 | 37.17 |
| **5** | 263 (1.02), 355 (0.95) | 550 | 496 | 0.19 | 0.43 | 5.1 | 36.56 |
| **6** | 261 (0.97), 351 (0.89) | 547 | 500 | 0.22 | 0.39 | 5.3 | 41.66 |

[a] In aerated $CH_2Cl_2$. [b] In aerated toluene ($\lambda_{ex} = 366$ nm).) [c] In butyronitrile glass at 77 K ($\lambda_{ex} = 366$ nm).) [d] In deaerated toluene; $\Phi$ versus *fac*-$Ir(ppy)_3$ in deaerated $CH_2Cl_2$ ($\Phi_{ref} = 0.40$). [e] The data for **1** are slightly different from those previously published [6], particularly for the lifetime, probably due to less efficient deareation in the previous experiments.

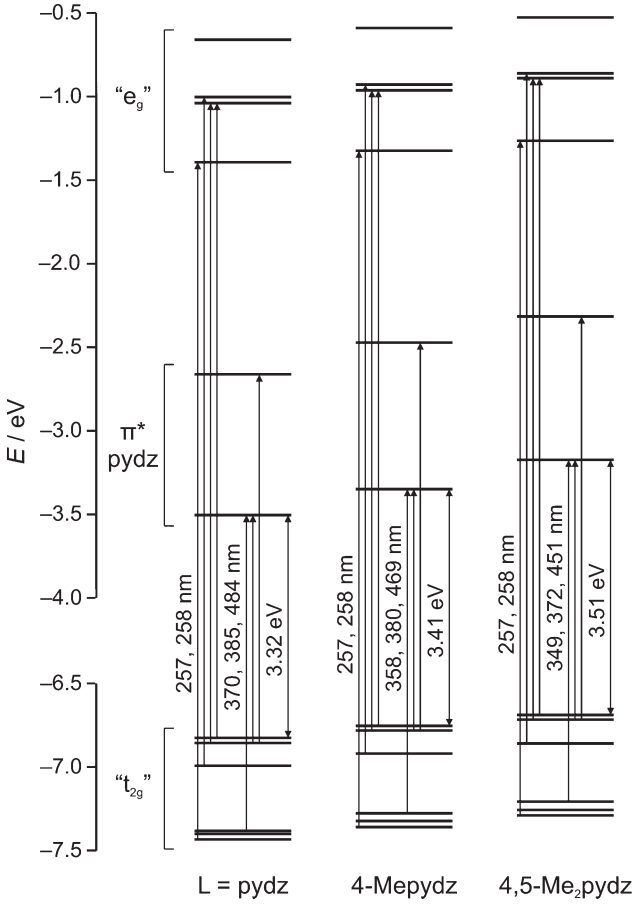


**Figure 3.** Partial molecular orbital diagrams for the complexes $[Re_2(\mu\text{-}Cl)_2(CO)_6(\mu\text{-}L)]$, L = pydz (**0**), 4-Mepydz (**1**), and 4,5-$Me_2$pydz (**4**). The electronic transitions responsible for the d–d and the MLCT absorption bands are highlighted, along with the HOMO–LUMO energy gap. The values reported were computed by TD DFT in the gas phase. Computations done in the presence of solvents of different polarity result in a qualitatively similar picture (values for dichloromethane and acetonitrile can be found in Table S3 of the Supporting Information).

The lower energy (351–364 nm) absorption bands have slightly weaker intensity ($\varepsilon \approx 0.81\text{–}0.94 \times 10^4\ M^{-1}\,cm^{-1}$) and can be assigned to singlet–singlet spin-allowed metal-to-ligand charge transfer transitions (MLCT), by analogy with the mononuclear tricarbonyl Re(I) complexes containing chelating diimine ligands. This assignment is also supported by the typical strong solvent dependence of the charge-transfer Re($\delta$)–L($\pi^*$) absorption band.[17] Indeed, as already reported for compound **0**,[6] a blue shift is observed upon increasing solvent polarity (from 371 nm in toluene to 336 nm in MeCN for **1**) (Fig. S4, Supporting Information). The position of the MLCT transition is dependent on the mono- or di-alkyl substitution on the aromatic ring. Going from **1–3** to **4–6**, the presence of two weak electron-donating groups makes charge transfer onto the substituted pyridazine more difficult, giving a blue shift in the absorption maxima (Fig. 2).

This trend nicely agrees with the variation of the electrochemical energy gap, $E_g$. Taking into account that the oxidation potential values are almost independent on the nature of the ligand, the observed decrease of the $\lambda_{abs}$ maximum could be attributed to the more negative reduction potential of the complexes containing dialkylated pyridazine. As evidenced by TD DFT computations[6] and illustrated in Figure 3, the electronic transitions responsible for the MLCT absorption band involve as starting orbitals the HOMO–1 and the HOMO–3 (i.e., not the HOMO) and as final orbitals both the two low lying $\pi^*$ orbitals of the diazine, LUMO and LUMO + 1 (i.e., not only the LUMO). However, according to the data reported in Table S4 of the Supporting Information for the three species **0**, **1**, and **4**, the shift in energy associated to the mono- and the dialkyl substitution at the $\beta$ position of the pyridazine ring is similar for LUMO and LUMO + 1 on one hand, and for HOMO, HOMO–1, and HOMO–3 on the other. As a consequence, a correlation between $\lambda_{abs}$ and $E_g$ can be evidenced (see Fig. S5, Supporting Information).

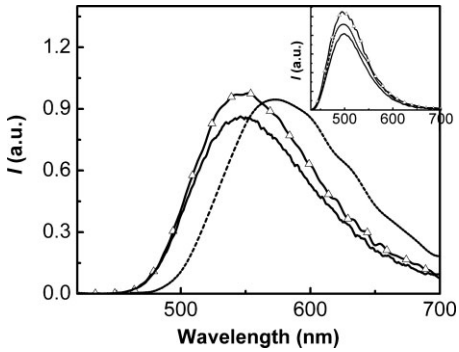


**Figure 4.** Emission spectra of complexes **1** (---), **4** (–△–) and **6** (—) in deaerated toluene at room-temperature ($\lambda_{ex}$ = 366 nm). Inset: emission spectra of complexes **1** (---), **4** (–△–) and **6** (—) in butyronitrile glass at 77 K ($\lambda_{ex}$ = 366 nm).

Upon excitation in the range 340–400 nm, all the complexes show bright, broad, and featureless emission in the green–yellow region of the visible spectrum (range 547–575 nm), at room temperature in diluted air-equilibrated and deaerated toluene solutions. The photoluminescence spectra for complexes **1**, **4**, and **6** are depicted in Figure 4 (the others are shown in Fig. S6 of the Supporting Information) and the data are summarized in Table 2. It has been checked that the emission is independent on the excitation wavelength and that all the complexes are photostable. The position of the emission is not affected by the nature of the alkyl substituents, but only by their number: the mono-alkylpyridazine complexes **1–3** show a $\lambda_{em}$ maximum at ca. 575 nm, while the disubstituted analogues emit at ca. 550 nm.

The excited state responsible for this intense emission can be confidently described as a triplet metal-to-ligand charge transfer ($^3$MLCT) level. The photoluminescence quantum yields (PLQY) are in the range 8–10% for the mono-alkylated derivatives, and 18–22% for the dialkylated ones. Taking into account that the pydz derivative emits at 600 nm with PLQY of ca. 5%,[6] it results that the introduction in the $\beta$ positions of each weak electron-donating alkyl group roughly doubles the PLQY and causes a blue shift of ca. 25 nm. These findings suggest a sort of additive effect of the substitution, both on the energy and on the intensity of the emission.

To the best of our knowledge, these PLQYs represent the *highest* values for *neutral* tricarbonyl Re(I) complexes.

The complexes showing the highest PLQYs (**4**–**6**) have also the longest emission lifetimes (Table 2). The values of $\Phi_{em}/\tau_{em}$ ($= k_r \times \eta_{isc}$, where the latter term represents the efficiency of the intersystem crossing process) are in the range 6.3–8.1 $\times 10^4$ $s^{-1}$. The $^3$MLCT nature of the transition involved in the emission is supported by the dioxygen quenching of the emission (see Table 2): on going from deaerated to aerated solutions, the lifetimes drop from 2–5 μs to ca. 0.4 μs, independent of the mono- or dialkyl substitution.

Low-temperature emission spectra and lifetimes were measured in butyronitrile rigid matrix at 77 K for all the complexes (Table 2). The emission bands (shown in the inset of Figure 4 for **1**, **4**, and **6**) maintain the structureless shape observed at room temperature, but their maxima display pronounced hypsochromic shifts. This rigido-chromism,[18] usually observed for emission from polar excited states, arises from the increase of the energy of the $^3$MLCT states, less stabilized by the lack of solvent mobility. The emission lifetimes in frozen conditions ($\tau_{em}$) are much longer than in the fluid state (30.9–41.7 μs), as expected by lowering the temperature. This behavior can be explained taking into account that a strong mixing of the $^3$MLCT and the triplet ligand centered, $^3$LC, states is possible at low temperature due to the rising in energy of the $^3$MLCT levels.[19]

The best performing complex, **6**, was selected for the construction of electroluminescent devices.

### 2.4. Electroluminescent Devices

Neutral rhenium complexes have been rarely employed in electroluminescent devices, either due to their very low emission quantum yields or their scarce solubility.[5] Furthermore, there are only few reports on OLEDs based on sublimation of such emitters.[4] To the best of our knowledge, thus far no comparison between devices made by sublimation and spin-coating has appeared in the literature for any type of rhenium compounds. We decided to compare such an electroluminescent behavior using the best photoluminescent complex, **6**, which is very soluble in organic solvents and is stable towards sublimation. It is also interesting to note that there is only one previous report concerning the use of a dinuclear rhenium complex in an electroluminescent device (which was solution-processed).[5b]

We built up polymer-based light-emitting diodes with **6** under inert conditions, using the studied compound as dopant in a poly(9-vinylcarbazole) (PVK) matrix. Devices were made with a layer of PEDOT:PSS acting as a hole-transporting material. The device structure can be represented as follows: glass/ITO/PEDOT:PSS (80 nm)/PVK + **6** (10 wt%) (60 nm)/TPBI (20 nm)/Ba (5 nm)/Al (80 nm) (full details about these acronyms are given in the Experimental Section).

The electroluminescence (EL) spectrum of the device with **6** is depicted in Figure 5. The EL maximum is centered at 550 nm and was only slightly shifted with respect to the photoluminescence spectrum (Table 2), indicating that the same optical transition is responsible for the light emission. The device showed weak voltage dependence. With increasing voltage, the EL did not increase dramatically while a weak emission resulting from the host polymer matrix was observed,[4a,5a,5e] suggesting that incomplete energy transfer from the host polymeric matrix to the guest rhenium complex takes place. The Commission International De L'Eclairage (CIE) coordinates of the emitted light are x = 0.40 and y = 0.54, corresponding to a yellow emission color as observed by eye.

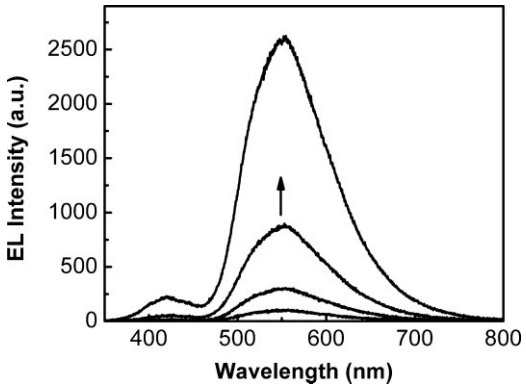


**Figure 5.** EL spectra with increased voltage from 12 V to 20 V of the solution-processed devices made with complex **6**.

Figure 6 presents the current–voltage and luminance–voltage characteristics of the device. The turn-on voltage ($V_{t\text{-}on}$), that is, the voltage needed to reach 1 cd $m^{-2}$, is in our device configuration about 12 V. The maximum luminance is 960 cd $m^{-2}$ at a driving voltage of 27 V. The value of maximum brightness observed for the EL devices studied in this paper is higher than the 121 cd $m^{-2}$ previously reported for an EL device based on the $Re(CO)_3Cl$-(mopvb) (mopvb = (trans-4-methyl-4′-(2-4-octadecyloxylphenyl)vinyl)-2,2′-bipyridine) complex incorporated into PVK host with a device configuration of ITO/PVK:$Re(CO)_3Cl$(mopvb)/BCP/LiF/Al (BCP = 2,9-dimethy-4,7-diphenyl-1,10-phenanthroline),[5f] and higher than 730 cd $m^{-2}$ for a Re complexes with 2,2′-bipyridine-5,5′-diyl with triphenylamine and 1,3,4-oxadiazole moietes doped in host material ofpolucarbonate (PC) with device struture of ITO/PVK: Re: PC/Al.[5d]

The device showed a maximum current efficiency of 2.03 cd $A^{-1}$ (0.34 lm $W^{-1}$) with a luminance of 40 cd $m^{-2}$ at a driving voltage of 18.5 V. The values of maximum current efficiency observed for the EL devices studied in this paper is close to the best previously reported value (2.1 cd $A^{-1}$).[5e] The external quantum efficiency (EQE) maximum of the device is around 0.6%, a value comparable

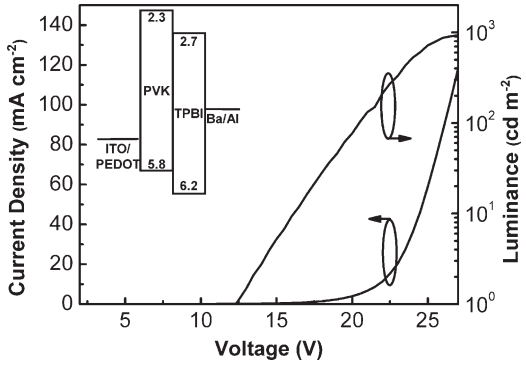


**Figure 6.** The *I*–*V*–*L* curves of the solution-processed device made with **6**. The structure of the device is shown in the inset.

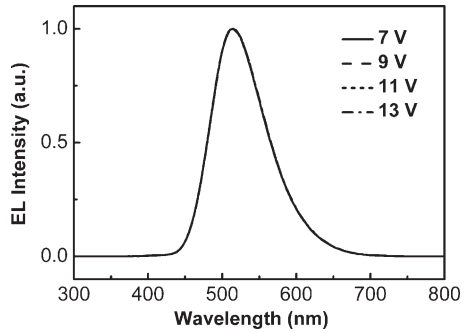


**Figure 7.** Electroluminescence spectra, at different bias, of a sublimation-processed device containing **6** in a PCF matrix.

to or even better than those reported for previous polymer-based neutral rhenium electroluminescent devices,[5] which encourages further studies of similar materials.

The same complex was employed to construct an OLED by vacuum sublimation. A light-emitting device with the configuration glass/ITO/NPB (30 nm)/PCF:7 wt% **6** (30 nm)/BCP (10 nm)/$Alq_3$ (30 nm)/LiF (10 Å)/Al (100 nm) was fabricated for this purpose. NPB and $Alq_3$ were utilized as hole- and electron-transport layers, respectively; BCP was employed as a simultaneous electron-transport and hole-block layer. Bipolar host material PCF[31], which features diphenylphosphine oxide groups appended to a carbazole/fluorene hybrid, was used as the host material for the rhenium complex. Figure 7 shows the corresponding EL spectrum at a bias of 7 V, with the CIE color coordinates of 0.26, 0.54 representing a green–yellow emission. To the best of our knowledge the emission of this device ($\lambda_{max} = 514$ nm) is the bluest ever reported for rhenium complexes. When we increased the driving voltage to 13 V, the CIE coordinates of the emission color remained almost constant and the EL spectrum did not change. The current density–voltage–luminance (*I–V–L*) characteristics of the PCF-based device are depicted in Figure 8. The device has a turn-on voltage of 4.1 V and, at a maximum luminance of 1 983 cd $m^{-2}$, its driving voltage was merely 12.5 V. These values are much lower than the driving voltages of the PVK-based device. We ascribe the reduced driving voltage of the PCF-based device to facile hole/electron injections within this bipolar host. The maximum current efficiency of 11.0 cd $A^{-1}$ (6.3 lm $W^{-1}$) was achieved at a luminance of 27 cd $m^{-2}$.

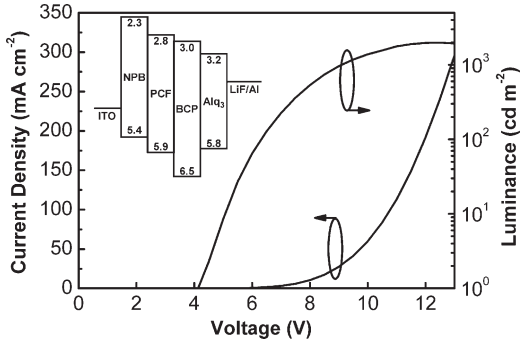


**Figure 8.** *I–V–L* curves of the device made by sublimation of complex **6** in a **PCF** matrix. The structure of the device is shown in the inset.

The EL efficiencies of this dinuclear rhenium-based device are amongst the highest reported for rhenium-based OLEDs. Notably, the current efficiency of the vacuum-deposited device was 5.5 times higher than that of its spin-coated counterpart. This large enhancement in device performance can be attributed to more balanced charge flux and better exciton confinement within the emission layer in vacuum-deposited device.

## 3. Conclusions

We have prepared a family of $[Re_2(\mu\text{-}Cl)_2(CO)_6(\mu\text{-diazine})]$ complexes, designed for optimizing the interaction energy and then reducing radiationless deactivation pathways. Our strategy results in air stable and highly emitting compounds. The emission quantum yields are much higher than usually observed for neutral Re(I) complexes. The good processability and solubility in organic solvents of these compounds, as well as their electrochemical properties encouraged their possible testing in electroluminescent devices and we made two types of OLED fabricated by solution processing and sublimation of the metal complex. The results obtained suggest that this class of triplet emitters can be processed in different ways and give similar emission energies for both types of devices. The electroluminescence obtained with the sublimed devices is one of the most efficient ever reported and such findings suggest that rhenium complexes could play an important role for the development of new triplet emitters for OLEDs.

## 4. Experimental

*Synthesis*: All the reactions were carried out under $N_2$ using the Schlenk technique. All the solvents were deoxygenated and dried by standard methods before use, while commercial deuterated solvents were used as received. $[ReCl(CO)_5]$ was prepared according to a literature method [20]. 4-methyl-pyridazine (Lancaster), hydrazine monohydrate (Fluka), 2-butyne (Fluka), formamidine acetate, 1-octyne, 2-hexyne, 3,3-dimethyl-1-butyne and 1-pyrrolidino-1-cyclopentene (all Aldrich) were used as received.

*Synthesis of the 1,2-diazines*: All the alkylated pyridazines, except the commercially available 4-methylpyridazine, were prepared according to a literature procedure, involving as first step the synthesis of 1,2,4,5-tetrazine (from hydrazine hydrate and formamidine acetate) and then its reaction with RCCR′ alkynes (see Figure 2) [10]. For the synthesis of 6,7-dihydro-5H-cyclopentapyridazine, tetrazine was reacted with 1-pyrrolidino-1-cyclopentene instead of the reactants used in the original work [10]. The purity of the ligands was checked by $^1$H-NMR spectroscopy.

*Synthesis of the Complexes 1–6*: The complexes (see Schemes 1 and 3 for their structures and abbreviations) were prepared from $[ReCl(CO)_5]$, using the method previously reported [6]. The crude products were purified by column chromatography (silica gel, $CH_2Cl_2$/*n*-hexane, 4:1), affording pure yellow powders in high isolated yields (50–60%).

*Characterization*: $^1$H-NMR spectra were recorded on a Bruker DRX400 spectrometer, in $CD_2Cl_2$ solution, at 300K. IR spectra were acquired on a Bruker Vector 22 FT instrument, in toluene solution. Elemental analyses were performed on a Perkin Elmer CHN2400 instrument.

*$[Re_2(\mu\text{-}Cl)_2(CO)_6(\mu\text{-4-methylpyridazine})]$ (1) [21]*: $^1$H-NMR: $\delta$ 2.68 (s, 3H, CH3), 7.86 (dd,1H), 9.64 (d, 1H, $J = 5.8$ Hz), 9.67 (d, $J = 1.3$ Hz, 1H). FT-IR $\nu$(CO) = 2050 (m), 2034 (s), 1947 (s), 1915 $cm^{-1}$ (s). Anal. calcd for $C_{11}H_6Cl_2N_2O_6Re_2$: C 18.73, H 0.86, N, 3.97; found: C 19.08, H 0.79, N 4.05.

*$[Re_2(\mu\text{-}Cl)_2(CO)_6(\mu\text{-4-n-hexylpyridazine})]$ (2)*: $^1$H-NMR: $\delta$ 0.94 (t, 3H, $CH_3$), 1.58–1.28 (br m, 6H, $CH_2CH_2CH_2$), 1.80 (quint, 2H, $CH_2$), 2.92 (t, 2H,$CH_3$), 7.84 (dd, 1H), 9.63 (d, $J = 1.2$ Hz, 1 H), 9.65 (d, $J = 5.8$ Hz, 1 H). FT-IR $\nu$(CO) = 2050 (m), 2034 (s), 1947 (s), 1915 $cm^{-1}$ (s). Anal. calcd for

$C_{16}H_{16}Cl_2N_2O_6Re_2$: C 24.78, H 2.08, N 3.61; found: C 25.08, H 1.93, N 3.61.

*[$Re_2(\mu$-Cl)$_2$(CO)$_6$($\mu$-4-ter-butylpyridazine)] (3)*: $^1$H-NMR: $\delta$ 1.53 (s, 9H, $C(CH_3)_3$), 7.95 (dd, 1H), 9.67 (dd, $J = 6.2$ Hz, 1H), 9.73 (dd, $J = 2.1$ Hz, 1H). FT-IR $\nu$(CO) = 2051 (m), 2034 (s), 1948 (s), 1916 cm$^{-1}$ (s). Anal. calcd for $C_{14}H_{12}Cl_2N_2O_6Re_2$: C 22.49, H 1.62, N 3.75%; found: C 22.63, H 1.65, N 3.71.

*[$Re_2(\mu$-Cl)$_2$(CO)$_6$($\mu$-4,5-dimethylpyridazine)] (4)*: $^1$H-NMR: $\delta$ 2.56 (s, 6H, $CH_3$), 9.50 (s, 2H). FT-IR $\nu$(CO) = 2050 (m), 2033 (s), 1946 (s), 1914 cm$^{-1}$ (s). Anal. calcd for $C_{12}H_8Cl_2N_2O_6Re_2$: C 20.03, H 1.12, N 3.89; found: C 20.49, H 1.25, N 3.84.

*[$Re_2(\mu$-Cl)$_2$(CO)$_6$($\mu$-4 methyl-5-propylpyridazine)] (5)*: $^1$H-NMR: $\delta$ 1.47 (t, 3H, $CH_3$), 1.79 (pt, 2H, $CH_2$), 2.59 (s, 3H, $CH_3$), 2.86 (t, 2H,$CH_2$), 9.45 (s, 1H), 9.49 (s, 1H). FT-IR $\nu$(CO) = 2050 (m), 2033 (s), 1947 (s), 1914 cm$^{-1}$ (s). Anal. calcd for $C_{14}H_{12}Cl_2N_2O_6Re_2$: C 22.49, H 1.62, N 3.75; found: C 22.75, H 1.60, N 3.65.

*[$Re_2(\mu$-Cl)$_2$(CO)$_6$($\mu$-6,7-dihydro-5H-cyclopentapyridazine)] (6)*: $^1$H-NMR: $\delta$ 2.42 (quint, 2H,$CH_2$), 3.27 (t, 4 H, -$CH_2$-$CH_2$-$CH_2$-), 9.67 (s, 2H). FT-IR $\nu$(CO) = 2050 (m), 2033 (s), 1946 (s), 1914 cm$^{-1}$ (s). Anal. calcd for $C_{13}H_8Cl_2N_2O_6Re_2$: C 21.34, H 1.10, N 3.83; found: C 21.56, H 1.24, N 3.68.

*Electrochemical Measurements*: The cyclovoltammetric study of the complexes was performed at scan rates typically ranging 0.02 to 10 V s$^{-1}$, in HPLC-grade $CH_3CN$ solutions at 0.00025–0.001 M concentration in each substrate, deareated by $N_2$ bubbling, with tetrabutylammonium hexafluorophosphate $TBAPF_6$ (Fluka) 0.1 M as the supporting electrolyte, at 298 K. The ohmic drop was compensated by the positive feedback technique [22]. The experiments were carried out using an AUTOLAB PGSTAT potentiostat (EcoChemie, The Netherlands) run by a PC with GPES software. The working electrode was a glassy carbon (AMEL, ø = 1.5 mm) cleaned by diamond powder (Aldrich, ø = 1 μm) on a wet cloth (STRUERS DP-NAP); the counter electrode was a Pt wire; the reference electrode was a saturated calomel electrode (SCE), having in our working medium a difference of –0.385 V vs. the $Fc^+|Fc$ couple (the intersolvental redox potential reference currently recommended by IUPAC)[23] and +0.032 V vs. the $Me_{10}Fc^+|Me_{10}Fc$ couple (an improved intersolvental reference under investigation) [24].

*Computational Details*: Geometries were optimized by means of density functional calculations. The parameter-free hybrid functional PBE0 [25] was employed along with the standard valence double-$\zeta$ polarized basis set 6-31G(d,p) for C, H, Cl, N, and O. For Re the Stuttgart–Dresden effective core potentials were employed along with the corresponding valence triple-$\zeta$ basis set. Dissociation and interaction energy values reported in the Supporting Information (Table S2) for compound **0**, **1**, and **4** are counterpoise corrected [26].

In order to simulate the absorption electronic spectrum down to 230 nm the lowest 30 singlet excitation energies were computed by means of time-dependent density functional calculations. Calculations were done also in the presence of solvent (dichloromethane and acetonitrile, Table S3) described by the conductor-like polarizable continuum model (CPCM) [27]. All the calculations were done with Gaussian 03 [28].

*Spectroscopy*: Absorption spectra were measured with a Varian Cary 5000 double-beam UV–Vis–NIR spectrometer and baseline corrected. Steady-state emission spectra were recorded on a HORIBA Jobin-Yvon IBH FL-322 Fluorolog 3 spectrometer equiped with a 450 W Xenon arc lamp, double grating excitation and emission monochromators (2.1 nm mm$^{-1}$; 1200 grooves mm$^{-1}$) and a Hamamatsu R928 photomultiplier tube. Emission and excitation spectra were corrected for source intensity (lamp and grating) and emission spectral response (detector and grating) by standard correction curves. Time-resolved measurements were performed using the time-correlated single-photon-counting (TCSPC) option on the Fluorolog 3. NanoLEDs (402 nm; FWHM < 750 ps) with repetition rates between 10 kHz and 1 MHz used to excite the sample. The excitation source were mounted on the sample chamber at 90° to a double grating emission monochromator (2.1 nm mm$^{-1}$ dispersion; 1200 grooves mm$^{-1}$) and collected by a TBX-4-X single-photon-counting detector. The photons collected at the detector were correlated by a time-to-amplitude converter (TAC) to the excitation pulse. Signals were collected using an IBH DataStation Hub photon counting module and data analysis was performed using the commercially available DAS6 software (HORIBA Jobin Yvon IBH). The goodness of fit was assessed by minimizing the reduced chi-square function ($\chi^2$) and visual inspection of the weighted residuals. Luminescence quantum yields ($\Phi_{em}$) were measured in optically dilute solution (optical density < 0.1 at the excitation wavelength) and compared to reference emitters by the method of Demas and Crosby [29]. The fac-Ir(ppy)$_3$ complex was used as reference in deaerated dichloromethane solution at room temperature ($\Phi_{em} = 0.40$) [30]. All the solvents were spectrophotometric grade and freshly distilled. Deaerated samples were prepared by the freeze-pump-thaw technique.

*OLED Preparation and Characterization; Spin-Coated Devices*: The solution processed devices were made using poly(9-vinylcarbazole) (PVK, $M_w = 1\,100\,000$), which was obtained from Aldrich. Poly(3,4-ethylenedioxythiophene): poly(styrenesulfonate) (PEDOT:PSS, 1: 6 dispersion in water, electronic grade AI4083) and 1,3,5-tris[*N*-(phenyl)benzimidazole]benzene (TPBI) were purchased from HC Starck and from Sensient Imaging Technologies, respectively.

The device structure consisted of a 120 nm transparent indium tin oxide (ITO) layer as the bottom electrode, supported on a glass substrate. The ITO was treated for 10 minutes with UV/$O_3$ (UVO Cleaner 144AX, Jelight Company) prior to any further processing. A 80 nm PEDOT:PSS layer was deposited, from a water solution of the polymer, on top of the ITO, using a spincoater P6700 from Specialty Coating Systems. The device was then annealed at 180 °C for 2 minutes. Then, the emissive layer was spin-coated from a $CH_2Cl_2$ solution containing 5 mg ml$^{-1}$ of PVK, 10 wt% of Re complex with respect to PVK mass. The polymer–$CH_2Cl_2$ solution was stirred at room temperature overnight before the Re complex addition. The PVK:Re complex in $CH_2Cl_2$ solution was stirred for a further hour at room temperature, and filtered through a 5 mm PTFE filter (Millex, Millipore) prior to spinning. To get a polymer layer with a thickness of 55–80 nm the solution was spin-coated (Delta6 RC spincoater from Suss Microtec) at 3 800 rpm (10 s), followed by 950 rpm (25 s). An electron-transport layer was prepared via thermal evaporation of TPBI (20 nm) at a pressure of 2.0–5.0 × 10$^{-6}$ mbar at a deposition rate of 2 Å s$^{-1}$ using a MBraun evaporation chamber. The barium electrode (5 nm) was evaporated on TPBI film in a vacuum chamber at a pressure of 2.0–5.0 × 10$^{-6}$ mbar at a rate of 2 Å s$^{-1}$. The aluminum top electrode (80 nm) was then immediately evaporated on top of the barium (5 nm) without reducing the vacuum.

All measurements were run in an inert atmosphere directly after device fabrication. Voltage scans were then performed from zero to a preset positive voltage and then back to zero. The OLEDs were characterized by attaching a computer-controlled low-noise single-channel direct-current (DC) power source that can act as both voltage source and current source, and a voltage meter or current meter (Keithley 2600, Keithley Instruments). Light from the diode was coupled to a photodiode and read out by an electrometer/high-resistance meter (Keithley 6517, Keithley Instruments). The output of the data was handled by a Labview (National Instruments)-based program. Calibration of the photodiode was done at a fixed current with a luminance meter (LS-100 Minolta). For every diode with a different spectral distribution of light, the photocurrent as measured by the photodiode was correlated to the light output in candles per square meter by this calibration. When recording an EL spectrum, a fiber-optic coupled spectrometer (USB2000, Ocean Optics) was used. The emission was corrected for the wavelength dependence of the spectrometer.

*Vacuum-deposited devices*: The host molecule 2,7-bis(diphenylphosphine oxide)-9-(9-phenylcarbazol-3-yl)-9-phenylfluorene (PCF) was prepared using previously reported procedures [31]. The hole-transport material 4,4′-bis[*N*-(1-naphthyl)-*N*-phenylamino]biphenyl (NPB), the hole-blocker 2,9-dimethy-4,7-diphenyl-1,10-phenanthroline (BCP), and the electron-transport material tris(8-hydroxyquinolinate) aluminum ($Alq_3$) were all purchased from LumTec Corp. and used without further purification.

The EL devices were fabricated through vacuum deposition (10$^{-6}$ torr) of the materials onto ITO glass (sheet resistance: 25 Ω square$^{-1}$). All of the organic layers were deposited at a rate of 1.0 Å s$^{-1}$. The cathode was completed through thermal deposition of LiF (10 Å; deposition rate: 0.1 Å s$^{-1}$) and then capping with Al metal (100 nm) through thermal

evaporation (deposition rate: 4.0 Å $s^{-1}$). The current density–voltage–luminance relationships of the devices were measured using a Keithley 2400 source meter and a Newport 1835C optical meter equipped with an 818ST silicon photodiode. The EL spectrum was obtained using a Hitachi F4500 spectrofluorimeter.

## Acknowledgements

G.D., M.P., D.D. and M.M. thank Italy's MIUR for financial support (FIRB 2003, RBNE033KMA, Molecular compounds and hybrid nanostructured material with resonant and nonresonant optical properties for photonic devices). L.D.C and Y.S thank Ciba for some financial support. Supporting Information is available online from Wiley InterScience or from the author.

Received: April 29, 2009
Published online: July 2, 2009

[1] M. A. Baldo, M. E. Thompson, S. R. Forrest, *Pure Appl. Chem.* **1999**, *71*, 2095.
[2] P.-T. Chou, Y. Chi, *Chem. Eur. J.* **2007**, *13*, 380.
[3] C. Adachi, M. A. Baldo, M. E. Thompson, S. R. Forrest, *J. Appl. Phys.* **2001**, *90*, 5048.
[4] For OLED devices, see for instance: a) Y. Li, Y. Liu, J. Guo, F. Wu, W. Tian, B. Li, Y. Wang, *Synth. Met.* **2001**, *118*, 175. b) X. Li, D. Zhang, W. Li, B. Chu, L. Han, J. Zhu, Z. Su, D. Bi, D. Wang, D. Yang, Y. Chen, *Appl. Phys. Lett.* **2008**, *92*, 83302. c) J. Li, Z. Si, C. Liu, C. Li, F. Zhao, Y. Duan, P. Chen, S. Liu, B. Li, *Semicond. Sci. Technol.* **2007**, *22*, 553. d) S. Ranjan, S.-Y. Lin, K.-C. Hwang, Y. Chi, W.-L. Ching, C.-S. Liu, y.-T. Tao, C.-H. Chien, S.-M. Peng, G.-H. Lee, *Inorg. Chem.* **2003**, *42*, 1248.
[5] For polymer light emitting devices see for instance: a) L. Qian, D. Bera, P. H. Holloway, *Appl. Phys. Lett.* **2007**, *90*, 103511. b) Y.-Y. Lü, C.-C. Jü, D. Guo, Z.-B. Deng, K.-Z. Wang, *J. Phys. Chem. C* **2007**, *111*, 5211. c) G. David, P. J. Walsh, K. C. Gordon, *Chem. Phys. Lett.* **2004**, *383*, 292. d) W. K. Chan, P. K. Ng, X. Gong, *Appl. Phys. Lett.* **1999**, *75*, 3920. e) Y. P. Wang, W. F. Xie, B. Li, W. L. Li, *Chin. Chem. Lett.* **2007**, *18*, 1501. f) B. Li, M. Li, Z. Hong, W. Li, T. Yu, H. Wei, *Appl. Phys. Lett.* **2004**, *85*, 4786.
[6] D. Donghi, G. D'Alfonso, M. Mauro, M. Panigati, P. Mercandelli, A. Sironi, P. Mussini, L. D'Alfonso, *Inorg. Chem.* **2008**, *28*, 4243.
[7] M. Panigati, D. Donghi, G. D'Alfonso, P. Mercandelli, A. Sironi, L. D'Alfonso, *Inorg. Chem.* **2006**, *26*, 10909.
[8] Instantaneous interaction energy ($\Delta E_{int}$) is the difference between the energy of the complex (ML) and that of the constituting metal and ligand fragments (M and L), computed employing the frozen geometry of the complex. A stronger metal–ligand interaction corresponds to a more negative interaction energy value.
[9] In particular, we found a stronger metal–ligand interaction on going from pyridazine to 4-methylpyridazine to 4,5-dimethylpyridazine ($\Delta E_{int} = -283$, $-288$ and $-293$ kJ $mol^{(1}$, respectively). More details can be found in the Supporting Information (Table S2).
[10] J. Sauer, D. K. Heldmann, J. Hetzenegger, J. Krauthan, H. Sichert, J. Schuster, *Eur. J. Org. Chem.* **1998**, 2885.
[11] These statements are based on the presence of symmetrical return peaks, the ≈57 mV half-peak widths, the nearly zero $E_p$ vs log $v$ slopes, as well as on the typical reversible peak morphological parameters.
[12] In the previous study it was shown that the position of the reduction peaks is well rationalized in terms of Hammett constants of the diazine substituents, giving a neat linear relationship with a rather high slope, on which the novel data here acquired nicely fit (Figure S1, Supporting Information).
[13] In particular, the $dE_p/d\log v$ slopes (Table S1, Supporting Information) are small but significant and the half-peak widths are higher than the expected 30 mV.
[14] A. J. Bard, L. R. Faulkner, in *Electrochemical Methods: Fundamentals and Applications*, Wiley, New York **2001**.
[15] J. M. Savéant, in *Elements of Molecular and Biomolecular Electrochemistry*, Wiley, New York **2006**.
[16] The symmetry labels "$t_{2g}$" and "$e_g$" are here used as an approximate description of the overall shape of the (mainly) metal-centered molecular orbitals. The actual symmetry of the species under study is lower than $O_h$ (in particular, it is $C_{2v}$ for **0** and **4**, and $C_s$ for **1**) and all the transitions described are indeed symmetry allowed. A list of all the excitations contributing to the bands discussed in the paper for compound **0**, **1**, and **4** are reported in the Supporting Information (Table S3), along with their description in terms of singly excited configurations. Both gas-phase and solution values are reported.
[17] P. J. Giordano, M. S. Wrighton, *J. Am. Chem. Soc.* **1979**, *101*, 2888.
[18] M. Wrighton, D. L. Morse, *J. Am. Chem. Soc.* **1974**, *96*, 998.
[19] P. J. Giordano, S. M. Fredericks, M. Wrighton, D. L. Morse, *J. Am. Chem. Soc.* **1978**, *100*, 2257.
[20] S. P. Schmidt, W. C. Trogler, F. Basolo, *Inorg. Synth.* **1985**, *23*, 41.
[21] The data for this compound have already been published [6] and are reported here for comparison.
[22] A. J. Bard, L. R. Faulkner, in *Electrochemical Methods: Fundamentals and Applications*, Wiley, New York **2002**, pp. 648.
[23] a) G. Gritzner, J. Kuta, *Pure Appl. Chem.* **1984**, *56*, 461. b) G. Gritzner, *Pure Appl. Chem.* **1990**, *62*, 1839.
[24] a) I. Noviandri, K. N. Brown, D. S. Fleming, P. T. Gulyas, P. A. Lay, A. F. Masters, L. Phillips, *J. Phys. Chem. B* **1999**, *103*, 6713. b) J. Ruiz, D. Astruc, *Comptes Rendus Acad. Sci, Série IIc: Chemie* **1998**, *I*, 21. c) L. Falciola, A. Gennaro, A. A. Isse, P. R. Mussini, M. Rossi, *J. Electroanal. Chem.* **2006**, *593*, 47.
[25] C Called PBE1PBE in Gaussian: a) C. Adamo, V. Barone, *J. Chem. Phys.* **1999**, *111*, 6158. b) J. P. Perdew, K. Burke, M. Ernzerhof, *Phys. Rev. Lett.* **1996**, *77*, 3865. c) J. P. Perdew, K. Burke, M. Ernzerhof, *Phys. Rev. Lett.* **1997**, *78*, 1396.
[26] N. R. Kestner, J. E. Combariza, in *Reviews in Computational Chemistry*, Vol. *13*(Eds: K. B. Lipkowitz, D. B. Boyd ), Wiley-VCH, New York **1999**, pp. 99–132.
[27] a) V. Barone, M. Cossi, *J. Phys. Chem. A* **1998**, *102*, 1995. b) M. Cossi, V. Barone, *J. Chem. Phys.* **2001**, *115*, 4708. c) M. Cossi, N. Rega, G. Scalmani, V. Barone, *J. Comput. Chem.* **2003**, *24*, 669.
[28] Gaussian 03, Revision C.02, M. J. Frisch, G. W. Trucks, H. B. Schlegel, G. E. Scuseria, M. A. Robb, J. R. Cheeseman, J. A. Montgomery, Jr., T. Vreven, K. N. Kudin, J. C. Burant, J. M. Millam, S. S. Iyengar, J. Tomasi, V. Barone, B. Mennucci, M. Cossi, G. Scalmani, N. Rega, G. A. Petersson, H. Nakatsuji, M. Hada, M. Ehara, K. Toyota, R. Fukuda, J. Hasegawa, M. Ishida, T. Nakajima, Y. Honda, O. Kitao, H. Nakai, M. Klene, X. Li, J. E. Knox, H. P. Hratchian, J. B. Cross, V. Bakken, C. Adamo, J. Jaramillo, R. Gomperts, R. E. Stratmann, O. Yazyev, A. J. Austin, R. Cammi, C. Pomelli, J. W. Ochterski, P. Y. Ayala, K. Morokuma, G. A. Voth, P. Salvador, J. J. Dannenberg, V. G. Zakrzewski, S. Dapprich, A. D. Daniels, M. C. Strain, O. Farkas, D. K. Malick, A. D. Rabuck, K. Raghavachari, J. B. Foresman, J. V. Ortiz, Q. Cui, A. G. Baboul, S. Clifford, J. Cioslowski, B. B. Stefanov, G. Liu, A. Liashenko, P. Piskorz, I. Komaromi, R. L. Martin, D. J. Fox, T. Keith, M. A. Al-Laham, C. Y. Peng, A. Nanayakkara, M. Challacombe, P. M. W. Gill, B. Johnson, W. Chen, M. W. Wong, C. Gonzalez, J. A. Pople, Gaussian, Inc, Wallingford CT **2004**.
[29] G. A. Crosby, J. N. C. Demas, *J. Am. Chem. Soc.* **1970**, *92*, 7262.
[30] A. B. Tamayo, B. D. Alleyne, P. I. Djurovich, S. Lamansky, I. Tsyba, N. N. Ho, R. Bau, M. E. Thompson, *J. Am. Chem. Soc.* **2003**, *125*, 7377.
[31] F.-M. Hsu, C.-H. Chien, P.-I. Shih, C.-F. Shu, *Chem. Mater.* **2009**, *21*, 1017.